Discovery of Novel Cdc25 Phosphatase Inhibitors with Micromolar Activity Based on the Structure-Based Virtual Screening

Hwangseo Park,*[,†] Young Jae Bahn,[‡] Suk-Kyeong Jung,[‡] Dae Gwin Jeong,[‡] Sang-Hyeup Lee,[‡] Il Seo,[‡] Tae-Sung Yoon,[‡] Seung Jun Kim,[‡] and Seong Eon Ryu*[,‡]

Department of Bioscience and Biotechnology, Sejong University, 98 Kunja-Dong, Kwangjin-Ku, Seoul 143-747, Korea, and Systemic Proteomics Research Center and Translational Research Center, Korea Research Institute of Bioscience and Biotechnology, 52 Eoeun-Dong, Yuseong-Gu, Daejeon 305-333, Korea

Received September 17, 2007

Cdc25 phosphatases have been considered as attractive drug targets for anticancer therapy because of the correlation of their overexpression with a wide variety of cancers. We have been able to identify five novel Cdc25 phosphatase inhibitors with micromolar activity by means of a computer-aided drug design protocol involving the homology modeling of Cdc25A and the virtual screening with the automated AutoDock program implementing the effects of ligand solvation in the scoring function. Because the newly discovered inhibitors are structurally diverse and reveal a significant potency with IC_{50} values lower than 10 μM, they can be considered for further development by structure−activity relationship studies or de novo design methods. The differences in binding modes of the identified inhibitors in the active sites of Cdc25A and B are discussed in detail.

Introduction

Cdc25 phosphatases belong to a class of dual-specificity phosphatase because they are able to dephosphorylate both a threonine and a tyrosine side chain of a protein substrate. Of the three Cdc25 homologues (Cdc25A, Cdc25B, and Cdc25C) encoded in human genome, Cdc25A and Cdc25B are shown to have oncogenic properties.[1] Cdc25A participates in the control of both G_1-to-S and G_2-to-S transitions in cell cycle by dephosphorylating and activating cyclin-dependent kinase (Cdk[a])/cyclin complexes, while Cdc25B is mainly involved in regulating the progression at the G_2-to-M transition.[2] Thus, Cdc25 phosphatases play a significant role in the regulation of the eukaryotic cell cycle progression by activating the Cdk/cyclins that serve as the central regulators of the cell cycle with the role of driving each state of cell division.

Owing to such an important contribution to the cell cycle regulation, Cdc25 phosphatases have been considered to be involved in oncogenic transformations and human cancers. The overexpression of Cdc25A and Cdc25B has been observed in a variety of tumor cells including breast cancer,[3] colon cancer,[4,5] non-Hodgkin's lymphoma,[6] prostate cancer,[7] pancreatic ductal adenocarcinoma,[8] and lung cancer.[9,10] Recent studies have also shown the involvement of Cdc25A in the adhesion-dependent proliferation of acute myeloid leukemia (AML) cells.[11] Further evidence for the oncogenic property of Cdc25 phosphatases was provided by the pharmacological studies in which the treatment of Cdc25 phosphatase inhibitors retarded the growth of the cancer cell lines expressing a high level of Cdc25 phosphatases.[12] It is now most likely that the overexpression of either Cdc25A or Cdc25B leads to the promotion of cell cycle progression in cancer cells although a simultaneous overexpression of both homologues was also observed in more aggressive cancers.[13] Thus, the inhibition of Cdc25 phosphatases may represent a novel approach for the development of anticancer therapeutics, although more details about the involvement of Cdc25A and Cdc25B overexpression in tumorigenesis remain to be clarified.

Structural investigations of Cdc25 phosphatases have lagged behind the mechanistic and pharmacological studies. So far, only two X-ray crystal structures of the catalytic domains of Cdc25A and Cdc25B have been reported in their ligand-free forms.[14,15] The lack of structural information about the nature of the interactions between Cdc25 phosphatases and small molecule inhibitors has made it a difficult task to discover a good lead compound for anticancer drugs. The structure-based design of Cdc25 inhibitors has also been hampered by the shallow active site region exposed to bulk solvent as well as the nucleophilic reactivity of the thiolate anion of the catalytic cystein residue. Nonetheless, a number of effective inhibitors of Cdc25 phosphatases have been discovered with structural diversity, as recently reviewed in a comprehensive manner.[16−18] Most of the Cdc25 inhibitors reported in the literature have stemmed from either the isolation of new scaffolds by high throughput screening[19] or the generation of the improved derivatives of pre-existing inhibitor scaffolds.[20−24] Binding modes of the newly found Cdc25 inhibitors have also been addressed with docking simulations in the active site to gain structural insight into their inhibitory mechanisms.[25−27]

In the present study, we apply a computer-aided drug design protocol involving the homology modeling, the structure-based virtual screening with docking simulations, and in vitro enzyme assay in a consecutive manner to identify novel classes of potent Cdc25 phosphatase inhibitors. Virtual screening has not always been successful because of the inaccuray in the scoring function that leads to a weak correlation between the enrichment in virtual screening and binding mode prediction.[28] The characteristic feature that disciriminates our virtual screening approach from the others lies in the implementation of an accurate solvation model in calculating the binding free energy between Cdc25 phosphatases and putative inhibitors, which would have the

* To whom correspondence should be addressed. For H.P.: phone, +82-2-3408-3766; fax, +82-2-3408-4334; e-mail, hspark@sejong.ac.kr. For S.E.R.: phone, +82-42-860-4149; fax, +82-42-860-4598; e-mail, ryuse@kribb.re.kr.

† Sejong University.

‡ Korea Research Institute of Bioscience and Biotechnology.

[a] Abbreviations: Cdk, cyclin-dependent kinase; AML, acute myeloid leukemia.

10.1021/jm701157g CCC: $40.75
Published on Web 08/21/2008

```
Cdc25A  332  DPRDLIGDFSKGYLFHTVAGKHQDLKYISPEIMASVLNGKFANLIKEFVIIDCRYPYEYE 391
Cdc25B  374  DHRELIGDYSKAFLLQTVDGKHQDLKYISPETMVALLTGKFSNIVDKFVIVDCRYPYEYE 433

Cdc25A  392  GGHIKGAVNLHMEEEVEDFLLKKPIVPTD-GKRVIVVFHCEFSSERGPRMCRYVRERDRL 450
Cdc25B  434  GGHIKTAVNLPLERDAESFLLKSPIAPCSLDKRVILIFHCEFSSERGPRMCRFIRERDRA 493

Cdc25A  451  GNEYPKLHYPELYVLKGGYKEFFMKCQSYCEPPSYRPMHHEDFKEDLKKFRTKSRTW    507
Cdc25B  494  VNDYPSLYYPEMYILKGGYKEFFPQHPNFCEPQDYRPMNHEAFKDELKTFRLKTRSW    550
```

Figure 1. Sequence alignment of the catalytic domains of Cdc25A and Cdc25B. The identity and the similarity between the corresponding residues are indicated in red and green, respectively. The residues constituting the active site are indicated in dotted rectangular box.

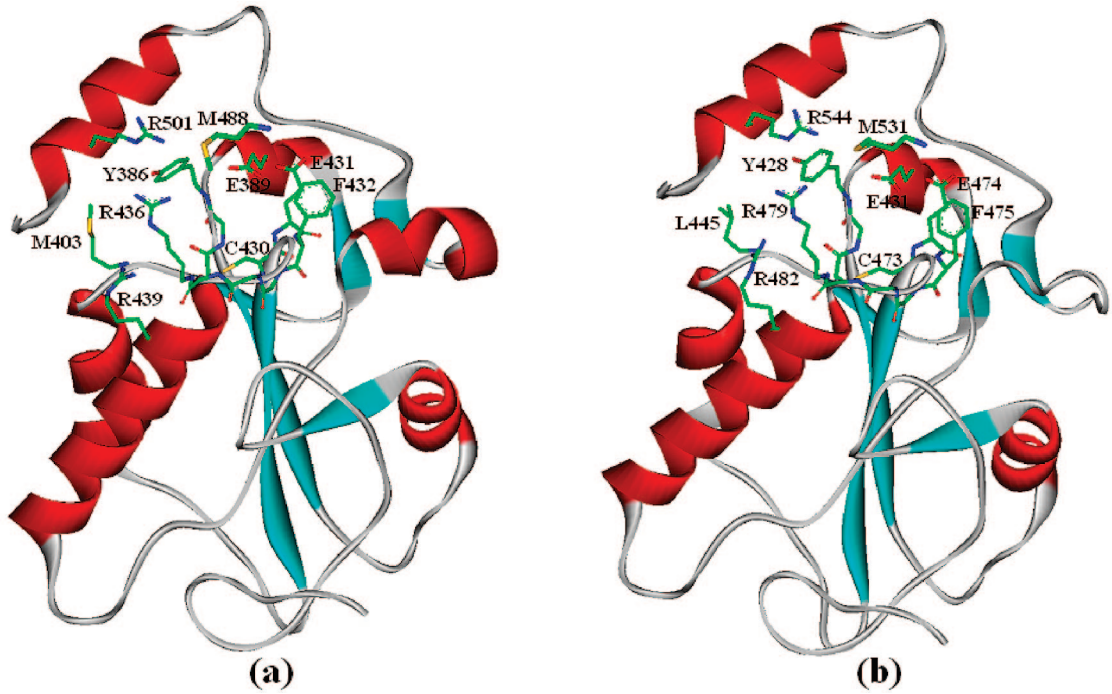

Figure 2. Comparative view of (a) the homology-modeled structure of Cdc25A and (b) the X-ray crystal structure of Cdc25B.

effect of hit rate in enzyme assay.[29,30] Cdc25A is selected as the target protein in virtual screening instead of Cdc25B because the former has not been considered in previous docking studies, and thus, the possibility of discovering the known inhibitors in a redundant manner should be reduced. The existing X-ray crystal structure of Cdc25A is inappropriate to be used in docking simulation of putative inhibitors because the active site region is maintained flat and exposed to bulk solvent in the crystallization conditions. Therefore, we use another conformation of Cdc25A suitable for structure-based virtual screening that is obtained from the homology modeling. To the best of our knowledge, we report the first example for the successful application of the structure-based virtual screening to identify novel Cdc25 phosphatase inhibitors. It will be shown that the docking simulation with the improved binding free energy function can be a valuable tool for enriching the chemical library with molecules that are likely to have biological activities as well as for elucidating the observed activity of the identified inhibitors.

Results and Discussion

Homology Modeling of Cdc25A. Although the X-ray structure of Cdc25A has been reported, it is inappropriate to be used in virtual screening because the active site region is maintained flat and exposed to bulk solvent. Therefore, a proper conformation of Cdc25A should be obtained from the homology modeling. Figure 1 displays the sequence alignment of the catalytic domains of Cdc25A and Cdc25B, which were used as the target and the template for homology modeling, respectively.[31] According to this alignment, the sequence identity and the similarity amount to 66.7% and 76.5%, respectively. Judging from such a high sequence homology, a high-quality 3D structure of Cdc25A can be obtained in the homology modeling. It is indeed well-known that the homology-modeled structure of a target protein can be accurate enough to be used in the structure-based ligand design as well as in the study of catalytic mechanism once the sequence identity between target and template exceeds 60%.[32] On the basis of the sequence alignment shown in Figure 1, 10 structural models of Cdc25A were calculated and the one with the lowest value of MODELLER objective function was selected as the final model of Cdc25A to be used in the subsequent virtual screening with docking simulations.

Figure 2 shows the structure of Cdc25A obtained from the homology modeling in comparison to the X-ray structure of Cdc25B that was used as the template. Of the 10 generated structural models of Cdc25A, some reveal a significantly different pattern for side chain packing when compared to the top-scored one. However, these structures were excluded in this study because they were poorly scored with a much larger MODELLER objective function than the best model. As expected from the high sequence identity, the target and the template possess a very similar folding structure and are superimposable over the main chain atoms. Despite the overall

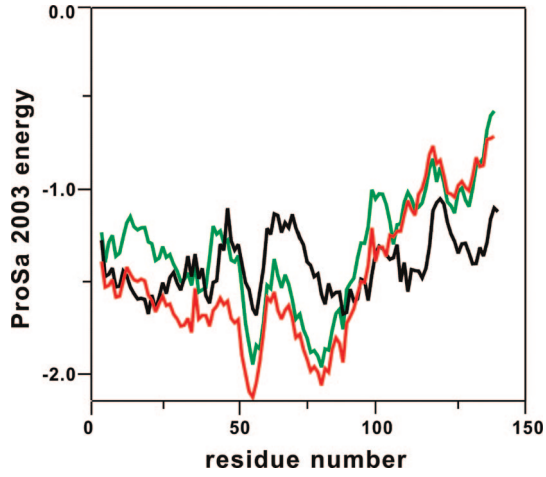

Figure 3. Comparison of ProSa energy profiles for the homology-modeled structure of Cdc25A (red) and the X-ray structures of Cdc25A (green) and Cdc25B (black). For convenience, the amino acids of both Cdc25 phosphatases are renumbered from 1 instead of retaining their original numbers.

structural similarity, however, two different structural features are observed around the active site. We first note that the residue Met403 near the active site of Cdc25A differs from the corresponding Leu445 in Cdc25B. As can be seen in Figure 2, the distances between the former and the neighboring active site residues (Arg436 and Arg501) are shorter than those between the latter and the corresponding Arg479 and Arg544 in the active site of Cdc25B. This difference has an effect of differentiating the accessibility of the active site between the two phosphatases. The second structural difference around the active sites is in the position of the Met residue located at the top of active site. Met488 points toward the cavity of the active site in Cdc25A, whereas the corresponding Met531 is directed outward to bulk solvent in Cdc25B. Owing to the two structural differences, the volume of the active site of Cdc25A is smaller than that of Cdc25B. Apparently, such a difference in active site geometry can serve as a clue for designing the selective Cdc25 phosphatase inhibitors.

The final structural model of Cdc25A obtained from the homology modeling was evaluated with the ProSa 2003 program by examining whether the interaction of each residue with the remainder of the protein is maintained as favorable. This program calculates the knowledge-based mean fields to judge the quality of protein folds and has been widely used to measure the stability of a protein conformation. Figure 3 shows the ProSa 2003 energy profile of the homology-modeled Cdc25A in comparison to those of the X-ray structures of Cdc25A and Cdc25B. We note that the ProSa energy remains negative for each amino acid residue in all three cases, indicating that all three protein structures should be acceptable. More interestingly, the homology-modeled structure of Cdc25A reveals a higher stability than the X-ray structure in most parts of the protein, further demonstrating the accuracy of the newly obtained structure of Cdc25A. This result also supports the possibility that the homology modeling with a high sequence identity and a high-quality template structure can produce a 3D structure of a target protein comparable in accuracy to the X-ray crystal structure.[32]

Virtual Screening and in Vitro Enzyme Assays. Of the 85 000 compounds subject to the virtual screening with docking simulation, 200 top-scored compounds were selected as virtual hits; 182 of them were available from the compound supplier and were tested for inhibitory activity against Cdc25 phosphatases by in vitro enzyme assays. As a result, we identified 16 compounds that inhibited the catalytic activity of one of the two Cdc25 phosphatases at least more than 50% at a concentration of 50 μM. Among them, the five compounds shown in Figure 4 were most potent with more than 70% inhibition at the same concentration and were selected to determine IC_{50} values. It is seen that three of the five inhibitors are similar in structure: 2-[4-allyl-5-(3-chlorophenyl)-4*H*-[1,2,4]triazol-3-ylsulfanyl]-1-(3,4-dihydroxyphenyl)ethanone **3** and 2-[4-(4-chlorophenyl)-5-*p*-tolyl-4*H*-[1,2,4]triazol-3-ylsulfanyl]-1-(3,4-dihydroxyphenyl)ethanone **4** have a common 1-phenyl-2-(5-phenyl-4*H*-[1,2,4]triazol-3-ylsulfanyl)ethanone scaffold, and the triazole moiety is replaced with the tetrazole ring in 1-(3,4-dihydroxyphenyl)-2-[2-(4-methoxyphenyl)-2*H*-tetrazol-5-ylsulfanyl]ethanone **2**. To the best of our knowledge, none of the five inhibitors have been reported as a Cdc25 inhibitor so far in the literature and patent. This indicates the usefulness of the homology-modeled structure of Cdc25A as an appropriate receptor model for the structure-based design of new Cdc25 phosphatase inhibitors. As shown in Table 1, all five inhibitors have a higher potency than the two known inhibitors, **6** (NSC 95397) and **7** (Cpd 5),[25] against both Cdc25 phosphatases with the IC_{50} values lower than 10 μM for Cdc25A. We note that the IC_{50} value of **6** determined in this study is higher than those obtained by the other groups; Lazo et al. reported that it was a submicromolar inhibitor,[25] whereas its IC_{50} value was in the micromolar range in another study.[23] These differences may be due to a strong dependence of the IC_{50} values on the experimental conditions of in vitro inhibition assay for Cdc25 phosphatases. It is also noteworthy that **2** and 2-{2-[5-(4-chlorophenyl)furan-2-yl]vinyl}-6-mercapto-4-oxo-1-phenyl-1,2,3,4-tetrahydropyrimidine-5-carbonitrile **5** exhibit about 4-fold higher activity against Cdc25A than against Cdc25B. The appearance of this selectivity is not surprising because the virtual screening was carried out using Cdc25A as the target protein. Judging from the novelty and the potency of the newly discovered inhibitors, they may deserve further development for anticancer drugs by structure−activity relationship or de novo design studies.

In order to provide experimental evidence for binding of the identified inhibitors in the active site of Cdc25 phosphatases, we have performed the steady-state kinetics evaluation of the inhibitors using Cdc25A and *O*-methylfluorescein phosphate as the target protein and the substrate, respectively. Compound **3** was excluded in this kinetic study because of its close structural similarity to the more potent inhibitor **4**. The 96-well microtiter plate assay was employed in this study using 30 mM Tris (pH 8.5), 75 mM NaCl, 1 mM EDTA, 1 mM DTT, and the reaction buffer of 0.033% BSA. The results of the kinetic studies are summarized in Figure 5. The Lineweaver−Burk plots indicate that all of the newly discovered inhibitors act like a competitive inhibitor of Cdc25A, suggesting that they inhibit the catalytic activity of Cdc25 phosphatases through the binding in the catalytic site. This allows the rationalization of the relative potencies of the inhibitors based on the comparison of their binding modes in the active site of Cdc25 phosphatases.

Molecular Modeling Studies of the Identified Inhibitors. To obtain some energetic and structural insight into the inhibitory mechanisms by the newly identified inhibitors of Cdc25 phosphatases, their binding modes in the active sites of Cdc25A and Cdc25B were investigated using the AutoDock program with the procedure described in Experimental Section. The calculated binding modes of the most potent inhibitor **4** in the active sites of the two Cdc25 phosphatases are compared in Figure 6. It is seen that the inhibitor is bound to the two

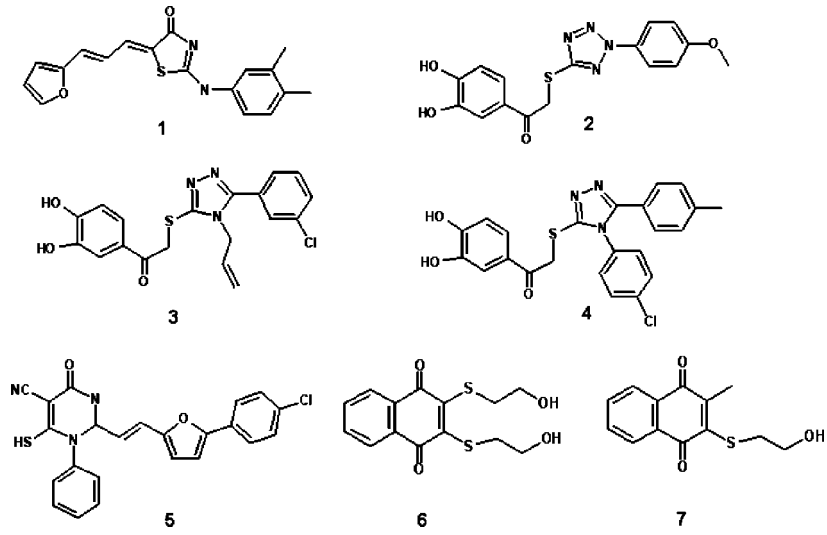

Figure 4. Chemical structures of the newly identified Cdc25 inhibitors (**1**−**5**) and the two known inhibitors (**6** and **7**).

Table 1. IC_{50} Values (in μM) of the Newly Identified Inhibitors **1**−**5** and the Two Known Inhibitors (**6** and **7**) against Cdc25 Phosphatases

inhibitors	Cdc25A	Cdc25B
1	4.27 ± 0.71	5.44 ± 0.19
2	4.07 ± 0.28	14.16 ± 0.67
3	3.28 ± 0.08	4.67 ± 0.42
4	0.82 ± 0.41	1.98 ± 0.44
5	3.31 ± 0.50	12.64 ± 0.37
6	5.49 ± 0.29	19.17 ± 0.33
7	4.56 ± 0.11	23.63 ± 0.80

homologues in different ways most probably because of the aforementioned difference in active site geometry. While both of the two phenolic oxygens are hydrogen-bonded to the side chain carboxylate groups of the two Glu residues (Glu474 and Glu431) in the active site in Cdc25B, only one forms a hydrogen bond with one Glu residue (Glu389) in that of Cdc25A. It is common to the two binding configurations that the inhibitor carbonyl group forms a hydrogen bond with a backbone amidic nitrogen. The presence of multiple hydrogen bonds in the two active sites indicates that the dihydroxyphenylcarbonyl moiety can play the role of anchor for binding of **4** in the active site of Cdc25 phosphatases. Although the triazole moiety of the inhibitor points outward and inward at the active sites of Cdc25A and Cdc25B, respectively, it is situated in the vicinity of the side chains of the catalytic Arg residues in both cases. Judging from the proximity to the Arg residues in the active site, the triazole moiety may serve as a surrogate for the substrate phosphate group. Another characteristic structural feature that discriminates the Cdc25A−**4** complex from the Cdc25B−**4** one lies in that the terminal toluene moiety is stabilized by hydrophobic interactions with the side chains of Trp507 and Arg501 in the former, whereas it is exposed to bulk solvent in the latter. The involvement of such hydrophobic interactions in the Cdc25A−**4** complex seems to compensate for the weakening of the hydrogen bond interactions compared to the Cdc25B−**4** complex, which can be an explanation for the little higher activity of **4** against Cdc25A than against Cdc25B.

To address the importance of the two active-site Glu residues in ligand binding, we carried out docking simulations of the inhibitor **4** in the active sites of mutant enzymes Cdc25A and B in comparison to the wild type Cdc25 phosphatases. Compound **4** was selected in this comparative analysis because it is most potent among the inhibitors found in this study. The mutations of E389 and E431 of Cdc25A into alanine lead to 1.2 and 0.8 kcal/mol increase in the binding free energy, respectively, when compared to that for **4** in the active site of wild type. Similarly, **4** is predicted to be less stabilized in the active site of E431A and E474A mutants of Cdc25B by 1.0 and 1.3 kcal/mol, respectively, than in the active site of the wild type. These results indicate the significant role of the two active-site Glu residues in the stabilization of the inhibitor through the formation of multiple hydrogen bonds.

Compound **2** possesses a tetrazole ring instead of the triazole as the surrogate for the substrate phosphate group and exhibits more than 3-fold higher inhibitory activity against Cdc25A than against Cdc25B. Therefore, a comparison of its binding modes in the two Cdc25 phosphatases is likely to be informative for designing selective inhibitors. Figure 7 shows the lowest-energy AutoDock conformations of **2** in the active sites of Cdc25A and Cdc25B. The calculated binding modes are similar to those of **4** in that the phenolic and carbonyl oxygens serve as the hydrogen bond donor and the acceptor with respect to the side chain carboxylate group of Glu residues and the backbone amidic nitrogen in the active site, respectively. This may be a confirmation for the role of anchor for binding played by the dihydroxyphenylcarbonyl moiety of the inhibitor. The tetrazole group of the inhibitor is stabilized by three Arg residues in the active site of Cdc25A with the two hydrogen bonds with Arg436 and Arg501, whereas it is directed to bulk solvent in Cdc25B. This indicates more stabilization of the inhibitor tetrazole group in the active site of Cdc25A, which may provide an explanation for the more than 3-fold higher inhibitory activity against Cdc25A. However, such a moderate selectivity of **2** for Cdc25A seems to be due to the formation of another hydrogen bond between the terminal anisole moiety and the side chain of Arg544 in the active site of Cdc25B, which can compensate in part for the absence of the interactions between the tetrazole moiety and the Arg residues.

In order to assess the roles of the active-site Arg residues of Cdc25A and B in the stabilization of **2**, we have performed the mutational analysis at positions 501 for Cdc25A and 544 for Cdc25B. The R501A and R501K mutants of Cdc25A and the corresponding R544A and R544K mutants of Cdc25B were constructed with the QuickChange site-directed mutagenesis kit (Stratagene) and confirmed by DNA sequence analysis. These Cdc25 phosphatase mutant proteins were purified by the same method as the wild types. Compared in Table 2 are the binding

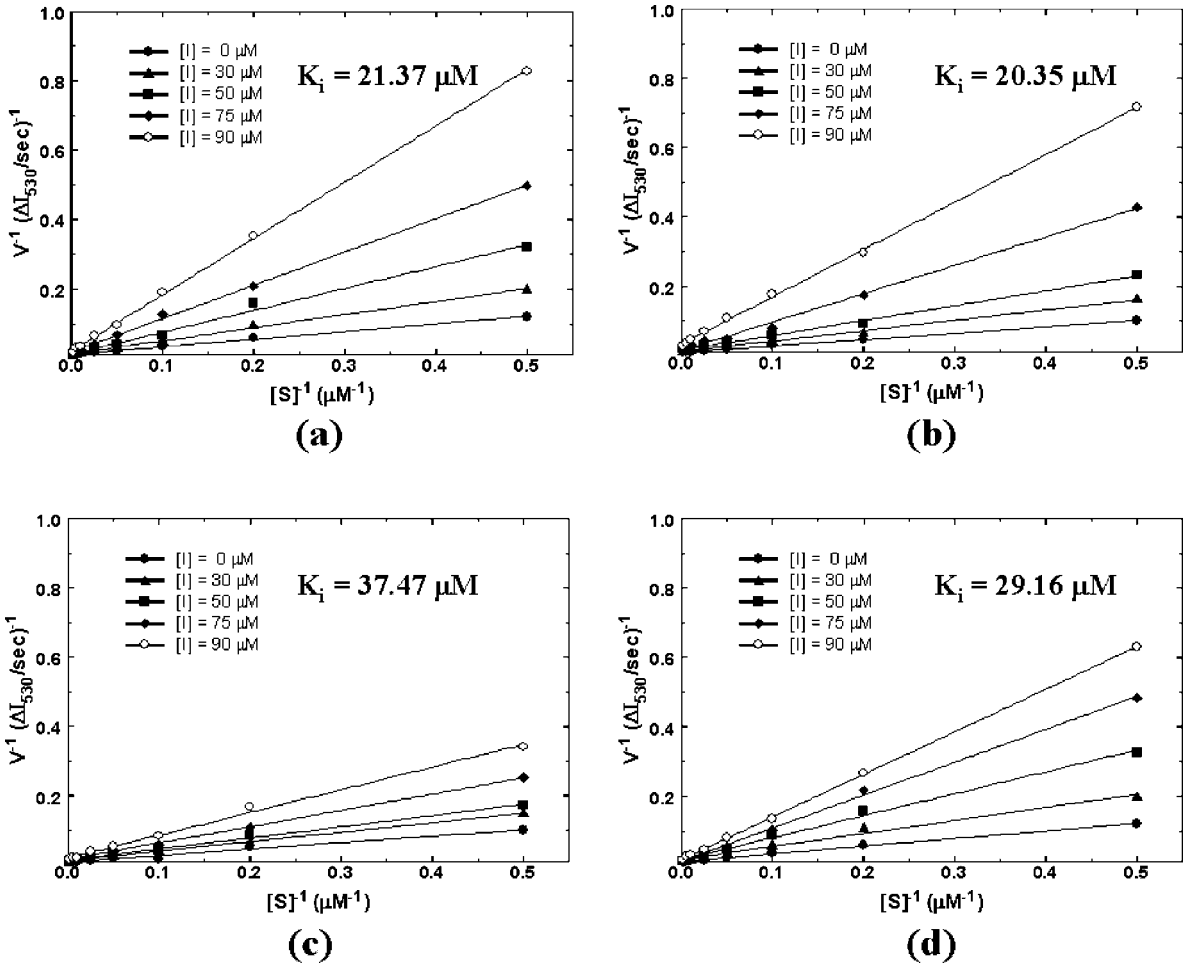

Figure 5. Lineweaver−Burk plots for the inhibition Cdc25A by (a) **1**, (b) **2**, (c) **4**, and (d) **5**. The concentrations of the inhibitors are 0, 30, 50, 75, and 90 μM. I_{530} is fluorescence intensity at 530 nm. The K_i values calculated from kinetic data are also indicated.

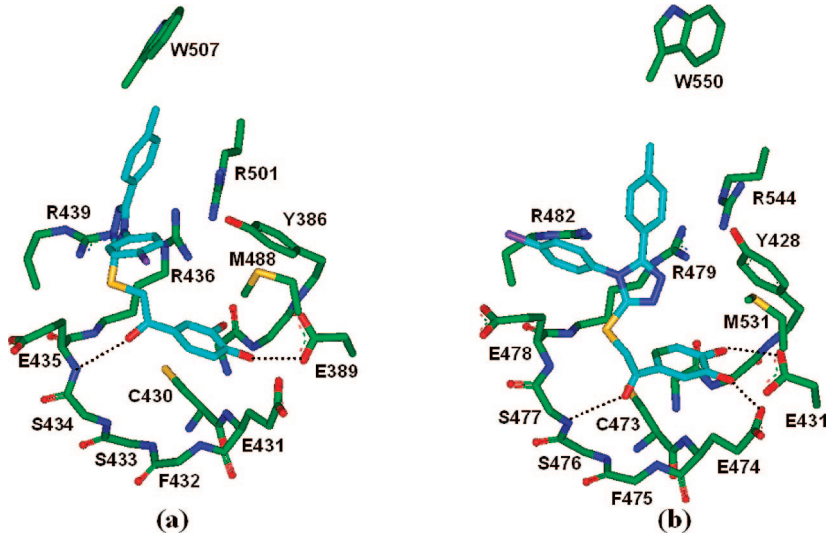

Figure 6. Calculated binding modes of **4** in the active sites of (a) Cdc25A and (b) Cdc25B. Carbon atoms of the protein and the ligand are indicated in green and cyan, respectively. Each dotted line indicates a hydrogen bond.

affinities of **2** for the wild-type Cdc25A and B with those for the mutants of Cdc25 phosphatases. We note that the mutation of Cdc25B at position 544 from Arg to Ala or Lys has little effect on the IC_{50} value of **2**, which indicates the insignificant role of Arg544 in the stabilization of **2** in the active site of Cdc25B. On the other hand, the IC_{50} value of **2** increases from 4 to 12 μM in going from wild type Cdc25A to the R501A mutant whereas it remains almost unchanged in the R501K mutant. This implies that **2** should be stabilized in the active site of Cdc25A through the interaction with a hydrogen-bond donating residue at position 501. These mutational analyses for Cdc25A and B are consistent with the above docking results indicating the greater hydrogen-bond stabilization of **2** by the positively charged residues in the active site of Cdc25A than

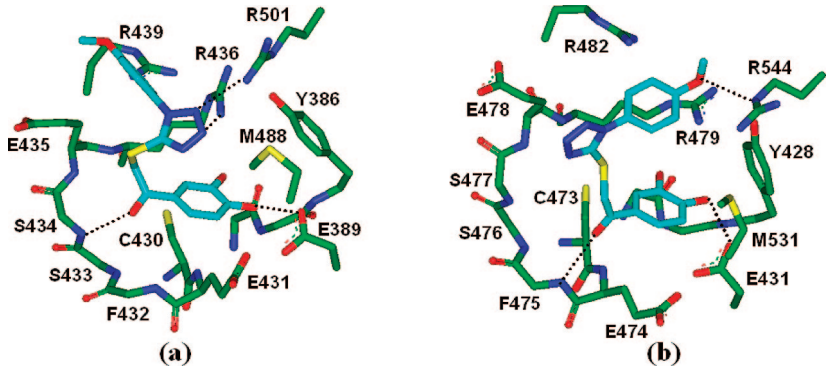

Figure 7. Calculated binding modes of **2** in the active sites of (a) Cdc25A and (b) Cdc25B. Carbon atoms of the protein and the ligand are indicated in green and cyan, respectively. Each dotted line indicates a hydrogen bond.

Table 2. IC_{50} Values (in μM) of **2** against the Wild-Type and Mutant Cdc25 Phosphatases

Cdc25A			Cdc25B		
wild type	R501A	R501K	wild type	R544A	R544K
4.07 ± 0.28	12.07 ± 0.46	6.09 ± 0.45	14.16 ± 0.67	16.02 ± 0.60	17.40 ± 0.32

in that of Cdc25B. Judging from the consistency between the experimental and computational results, the capability of forming a hydrogen bond with the active-site Arg residue is likely to serve as a determinant for the selectivity of Cdc25 phosphatases.

2-(3,4-Dimethylphenylamino)-5-(3-furan-2-ylallylidene)thiazol-4-one **1** exhibits similar inhibitory activity against Cdc25A and Cdc25B. Its binding modes in the active sites of the two Cdc25 phosphatases are compared in Figure 8. We note that the furan ring of **1** is situated deep in the active site of Cdc25B while it resides at the entrance of active site in Cdc25A. A difference in binding modes is also observed in the pattern for hydrogen bond formation; **1** forms two hydrogen bonds with the backbone amidic nitrogen in the active site of Cdc25B compared to only one in that of Cdc25A. These structural features indicate a higher inhibitory activity of **1** against Cdc25B. However, the terminal *o*-xylene moiety of the inhibitor is stabilized in Cdc25A by hydrophobic interactions with the side chains of Met403, Glu404, and Ser504, whereas it is exposed to bulk solvent in the Cdc25B−**1** complex. Thus, the involvement of a stronger hydrophobic interaction in Cdc25A-**1** than in Cdc25B-**1** can be an explanation for the similar potency of **1** for the two Cdc25 phosphatases.

As a check for the accuracies of the calculated binding modes of the newly identified inhibitors in the active sites of Cdc25 phosphatases, the flexible docking simulations were carried out with AutoDock 4 in which the motional flexibilities of the side chains shown in Figures 6−8 were taken into account. The binding configurations obtained from the precedent docking simulations were used as the starting structures. The results show that the root-mean-square deviation of the binding configuration from the initial structure remains within 1.2 Å in all six cases, which supports the plausibility of the calculated binding modes described above. A similar binding mode was also proposed for vitamin K derivative inhibitors in which the surrogate group for the substrate phosphate moiety proved to be stabilized near the catalytic cysteine residue through the formation of multiple hydrogen bonds in the active site.[27] Thus, it is demonstrated in this study that the docking simulation with the improved binding free energy function can be a useful tool for elucidating the observed activities of the identified inhibitors.

Experimental Section

Homology Modeling of Cdc25A. Although the X-ray crystal structure of Cdc25A has been reported in a ligand-free form,[14] it is inappropriate to be used in docking simulation of putative inhibitors because the active site region is maintained flat and exposed to bulk solvent in the crystallization condition. In order to obtain another conformation of Cdc25A suitable for structure-based virtual screening, we therefore carried out the homology modeling using the X-ray structure of Cdc25B as a template. This homology modeling started with the retrieval of the peptide sequence of human Cdc25A comprising 524 amino acid residues from the SWISS-PROT protein sequence data bank (http://www.expasy.org/sprot/; accession number P30304).[33] Sequence alignment between the catalytic domains of Cdc25A and Cdc25B was then derived with the ClustalW package[34] using the BLOSUM matrices for scoring the alignments. The parameters of GAP OPEN, GAP EXTENTION, and GAP DISTANCE were set equal to 10, 0.05, 8, respectively. Opening and extension gap penalties were thus changed systematically, and the obtained alignment was inspected for violation of structural integrity in the structurally conserved regions. On the basis of the best-scored sequence alignment, the three-dimensional structure of the catalytic domain of Cdc25A was constructed using the MODELLER 6v2 program.[35] In this model building, we employed an optimization method involving conjugate gradients and molecular dynamics to minimize the violations of the spatial restraints. With respect to the structure of gap regions, the coordinates were built from a randomized distorted structure that is located approximately between the two anchoring regions as implemented in MODELLER 6v2. To increase the accuracy of calculated structure, the loop modeling was also performed with the enumeration algorithm.[36] Then we calculated the conformational energy of the predicted structure of Cdc25A with ProSa 2003 program[37] for the purpose of evaluation.

Virtual Screening of Cdc25 Phosphatase Inhibitors. We used the AutoDock program[38] in the structure-based virtual screening of Cdc25 phosphatase inhibitors because the outperformance of its scoring function over those of the others had been shown in several target proteins.[39] The atomic coordinates of Cdc25A obtained from the homology modeling were used as the receptor model in the virtual screening with docking simulations. Special attention was paid to assign the protonation states of the ionizable Asp, Glu, His, and Lys residues. The side chains of Asp and Glu residues were assumed to be neutral if one of their carboxylate oxygens pointed toward a hydrogen-bond accepting group including the backbone aminocarbonyl oxygen at a distance within 3.5 Å, a generally accepted distance limit for a hydrogen bond of moderate strength.[40] Similarly, the lysine side chains were protonated unless the NZ atom was in proximity to a hydrogen-bond donating group. The same procedure was also applied to determine the protonation states of ND and NE atoms in His residues. The catalytic cysteine residues

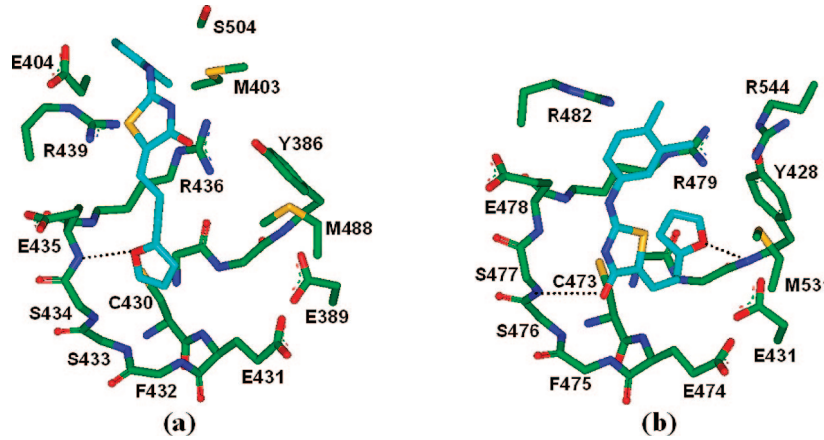

Figure 8. Calculated binding modes of **1** in the active sites of (a) Cdc25A and (b) Cdc25B. Carbon atoms of the protein and the ligand are indicated in green and cyan, respectively. Each dotted line indicates a hydrogen bond.

were set to be deprotonated in both Cdc25 phosphatases to be consistent with its role of nucleophile in the catalytic mechanism. The neighboring Glu residues (Glu431 of Cdc25A and Glu474 of Cdc25B) were assumed to be ionized because of the presence of hydrogen-bond donating groups and the absence of any hydrogen-bond accepting group in the vicinity of the two carboxylate oxygens in both homology-modeled structure of Cdc25A and X-ray structure of Cdc25B.

The docking library for Cdc25A comprising about 85 000 compounds was constructed from the latest version of Interbioscreen database (http://www.ibscreen.com) containing approximately 30 000 natural and 290 000 synthetic compounds. This selection was based on druglike filters that adopt only the compounds with physicochemical properties of potential drug candidates[41] and without reactive functional group(s). All of the compounds included in the docking library were then subjected to the Corina program to generate their three-dimensional atomic coordinates, followed by the assignment of Gasteiger−Marsilli atomic charges.[42] Docking simulations with AutoDock were then carried out in the active site of Cdc25A to score and rank the compounds in the docking library according to the binding affinity for Cdc25A.

In the actual docking simulation of the compounds in the docking library, we used the empirical AutoDock scoring function improved with a new solvation model for a compound. The modified scoring function has the following form:

$$\Delta G_{\mathrm{bind}}^{\mathrm{aq}} = W_{\mathrm{vdW}} \sum_{i=1} \sum_{j>i} \left(\frac{A_{ij}}{r_{ij}^{12}} - \frac{B_{ij}}{r_{ij}^{6}} \right) + W_{\mathrm{hbond}} \sum_{i=1} \sum_{j>i} E(t) \left(\frac{C_{ij}}{r_{ij}^{12}} - \frac{D_{ij}}{r_{ij}^{10}} \right) + W_{\mathrm{elec}} \sum_{i=1} \sum_{j>i} \frac{q_i q_j}{\varepsilon(r_{ij}) r_{ij}} + W_{\mathrm{tor}} N_{\mathrm{tor}} + W_{\mathrm{sol}} \sum_{i=1} S_i \left(\mathrm{Occ}_i^{\max} - \sum_{j>i} V_j e^{-r_{ij}^2/(2\sigma^2)} \right) \quad (1)$$

where W_{vdW}, W_{hbond}, W_{elec}, W_{tor}, and W_{sol} are weighting factors of van der Waals, hydrogen bond, electrostatic interactions, torsional term, and desolvation energy of inhibitors, respectively. r_{ij} represents the interatomic distance, and A_{ij}, B_{ij}, C_{ij}, and D_{ij} are related to the depths of energy well and the equilibrium separations between the two atoms. The hydrogen bond term has an additional weighting factor, $E(t)$, representing the angle-dependent directionality. With respect to the distant-dependent dielectric constant, $\varepsilon(r_{ij})$, a sigmoidal function proposed by Mehler et al.[43] was used in computing the interatomic electrostatic interactions between the receptor protein and its putative ligands. In the entropic term, N_{tor} is the number of rotatable bonds in a ligand. In the desolvation term, S_i and V_i are the solvation parameter and the fragmental volume of atom i,[44] respectively, while $\mathrm{Occ}_i^{\max}$ stands for the maximum atomic occupancy. In the calculation of molecular solvation free energy term in eq 1, we used the atomic parameters recently developed by Kang et al.[45] because those of the atoms other than carbon were unavailable in the current version of AutoDock. This modification of the solvation free energy term is expected to increase the accuracy in virtual screening because the underestimation of ligand solvation often leads to the overestimation of the binding affinity of a ligand with many polar atoms.[30]

The docking simulation of a compound in the docking library started with the calculation the 3D grids of interaction energy for all of the possible atom types present in chemical database. These uniquely defined potential grids for the receptor protein were then used in common for docking simulations of all compounds in the docking library. For the center of the common grids in the active site, we used the center of mass coordinates of the docked structure of **6**, whose binding mode in the active site of Cdc25B had been widely investigated by a variety of docking simulations.[25−27] The calculated grid maps were of dimension 61 × 61 × 61 points with the spacing of 0.375 Å, yielding a receptor model that includes atoms within 22.9 Å of the grid center. For each compound in the docking library, 10 docking runs were performed with the initial population of 50 individuals. Maximum number of generations and energy evaluation were set to 27 000 and 2.5×10^5, respectively. Docking simulations with AutoDock were then carried out in the active site of Cdc25A to score and rank the compounds in the docking library according to the binding affinity for Cdc25A.

In Vitro Enzyme Assay. The catalytic domains of the two Cdc25 phosphatases (Cdc25A, residues 336−523; Cdc25B, residues 378−566) were overexpressed in *E. coli* by using pET28a (Novagen) with 6xHis tag in the N-terminus. The overexpressed Cdc25 phosphatases were purified by Ni-NTA affinity resin (Qiagen) and frozen (−75 °C) in a buffer containing 20 mM Tris-HCl, pH8.0, 0.2 M NaCl, and 5 mM DTT until enzyme assay. In the phosphatase assay using 96-well plates, the reaction mixture included 180 μL of reaction buffer (20 mM Tris-HCl, pH 8.0, 0.01% Triton X-100, 5 mM DTT) with 10 μM 6,8-difluoro-4-methylumbelliferyl phosphate (DiFMUP, Molecular Probe), 10 μL of enzyme (30nM Cdc25A or 20nM Cdc25B), and 10 μL of a DMSO dissolved inhibitor. The reaction was performed for 20 min at room temperature and stopped by adding 1 mM sodium orthovanadate (final concentration). The fluorescence was measured (355 nm excitation and 460 nm emission) by a plate reader. IC_{50} values were estimated at least three times, and the averaged values were used in Table 1. As the positive controls for the enzyme inhibition assay, we used **6** and **7** shown in Figure 4. These compounds have micromolar inhibitory activity against Cdc25 phosphatases and are known to be one of the most potent growth inhibitors of various tumor cell lines.[46,47] The steady-state kinetic evaluations of compounds **1**, **2**, **4**, and **5** were performed using Cdc25A and *O*-methylfluorescein phosphate as the target protein and the substrate, respectively. The 96-well microtiter plate assay developed

by Rice et al.[48] was employed in this study using 30 mM Tris (pH 8.5), 75 mM NaCl, 1 mM EDTA, 1 mM DTT, and the reaction buffer of 0.033% BSA. The concentrations of the inhibitors were 0, 30, 50, 75, and 90 μM. The concentration of product was monitored by the intensity of fluorescence (480 nm excitation and 530 nm emission). The resulting kinetic data were then converted to Lineweaver−Burk plots.

Conclusions

We have identified five new novel inhibitors of Cdc25 phosphatases by applying a computer-aided drug design protocol involving the homology modeling of Cdc25A and the structure-based virtual screening with the automated AutoDock program implementing the effects of ligand solvation in the scoring function. These inhibitors are structurally diverse and exhibit a significant potency with IC_{50} values ranging from 0.8 to 15 μM. Therefore, the newly discovered inhibitors can provide the new scaffolds for further development of anticancer drugs by structure−activity relationship studies or de novo design methods. It is shown from a detailed binding mode analysis with docking simulation that the binding of the inhibitors in the active site of Cdc25B can be facilitated by the establishment of multiple hydrogen bonds with the side chain and backbone groups. The formation of such hydrogen bonds becomes less favorable in the case of Cdc25A because of the decrease in active site volume. For this reason, the hydrophobic interactions with the residues near the active site can also play a significant role in stabilizing the inhibitors in the active site of Cdc25A. This may serve as key information for future designing of the selective Cdc25 inhibitors. The present study demonstrates the usefulness of the automated AutoDock program with the improved scoring function as a new docking tool for virtual screening as well as for binding mode analysis to elucidate the activities of identified inhibitors.

Acknowledgment. This work was supported by the grant from KRIBB Research Initiative Program. The authors thank Prof. Seung W. Ham at Chung-Ang University for providing compounds **6** and **7**.

References

(1) Kristjansdottir, K.; Rudolph, J. Cdc25 phosphatases and cancer. *Chem. Biol.* **2004**, *11*, 1043–1051.
(2) Rudolph, J. Cdc25 phosphatases: structure, specificity, and mechanism. *Biochemistry* **2007**, *46*, 3595–3604.
(3) Galaktionov, K.; Lee, A. K.; Eckstein, J.; Draetta, G.; Meckler, J.; Loda, M.; Beach, D. Cdc25 phosphatases as potential human oncogenes. *Science* **1995**, *269*, 1575–1577.
(4) Hernández, S.; Bessa, X.; Beá, S.; Hernández, L.; Nadal, A.; Mallofré, C.; Muntane, J.; Castells, A.; Fernández, P. L.; Cardesa, A.; Campo, E. Differential expression of Cdc25 cell-cycle-activating phosphatases in human colorectal carcinoma. *Lab. Invest.* **2001**, *81*, 465–473.
(5) Takemara, I.; Yamamoto, H.; Sekimoto, M.; Ohue, M.; Noura, S.; Miyake, Y.; Matsumoto, T.; Aihara, T.; Tomita, N.; Tamaki, Y.; Sakita, I.; Kikkawa, N.; Matsuura, N.; Shiozaki, H.; Monden, M. Overexpression of Cdc25B phosphatase as a novel marker of poor prognosis of human colorectal carcinoma. *Cancer Res.* **2000**, *60*, 3043–3050.
(6) Hernandez, S.; Hernandez, L.; Bea, S.; Pinyol, M.; Nayach, I.; Bellosillo, B.; Nadal, A.; Ferrer, A.; Fernandez, P. L.; Montserrat, E.; Cardesa, A.; Cardes, E.; Campo, E. Cdc25A and the splicing variant Cdc25B2, but not Cdc25B1, -B3 or -C, are overexpressed in aggressive human non-Hodgkin's lymphomas. *Int. J. Cancer* **2000**, *89*, 148–152.
(7) Ngan, E. S. W.; Hashimoto, Y.; Ma, Z.-Q.; Tsai, M. J.; Tsai, S. Y. Overexpression of Cdc25B, an androgen receptor coactivator, in prostate cancer. *Oncogene* **2003**, *22*, 734–739.
(8) Guo, J.; Kleeff, J.; Li, J.; Ding, J.; Hammer, J.; Zhao, Y.; Giese, T.; Korc, M.; Büchler, M. W.; Friess, H. Expression and functional significance of Cdc25B in human pancreatic ductal adenocarcinoma. *Oncogene* **2004**, *23*, 71–81.
(9) Wu, W. G.; Fan, Y. H.; Kemp, B. L.; Walsh, G.; Mao, L. Overexpression of Cdc25A and cdc25B is frequent in primary nonsmall cell lung cancer but is not associated with overexpression of c-myc. *Cancer Res.* **1998**, *58*, 4082–4085.
(10) Sasaki, H.; Yukiue, H.; Kobayashi, Y.; Tanahashi, M.; Moriyama, S.; Nakashima, Y.; Fukai, I.; Kiriyama, M.; Yamakawa, Y.; Fujii, Y. Expression of the Cdc25B gene as a prognosis marker in non-small cell lung cancer. *Cancer Lett.* **2001**, *173*, 187–192.
(11) Fernandez-Vidal, A.; Ysebaert, L.; Didier, C.; Betous, R.; Toni, F. D.; Prade-Houdellier, N.; Demur, C.; Contour-Galcéra, M.-O.; Prévost, G. P.; Ducommun, B.; Payrastre, B.; Racaud-Sultan, C.; Manenti, S. Cell adhesion regulates Cdc25A expression and proliferation in acute myeloid leukemia. *Cancer Res.* **2006**, *66*, 7128–7135.
(12) Nishikawa, Y.; Carr, B. I.; Wang, M.; Kar, S.; Finn, F.; Dowd, B.; Zheng, Z. B.; Kerns, J.; Naganathan, S. Growth inhibition of hepatoma cells induced by vitamin K and its analogs. *J. Biol. Chem.* **1995**, *270*, 28304–28310.
(13) Boutros, R.; Dozier, C.; Ducommun, B. The when and wheres of Cdc25 phosphatases. *Curr. Opin. Cell Biol.* **2006**, *18*, 185–191.
(14) Fauman, E. B.; Cogswell, J. P.; Lovejoy, B.; Rocque, W. J.; Holmes, W.; Montana, V. G.; Piwnica-Worms, H.; Rink, M. J.; Saper, M. A. Crystal structure of the catalytic domain of the human cell cycle control phosphatase, Cdc25A. *Cell* **1998**, *93*, 617–625.
(15) Reynolds, R. A.; Yem, A. W.; Wolfe, C. L.; Deibel, M. R.; Chidester, C. G.; Watenpaugh, K. D. Crystal structure of the catalytic subunit of Cdc25B required for G_2/M phase transition of the cell cycle. *J. Mol. Biol.* **1999**, *293*, 559–568.
(16) Contour-Galcéra, M.-O.; Sidhu, A.; Prévost, G.; Bigg, D.; Ducommun, B. What's new on Cdc25 phosphatase inhibitors. *Pharmcol. Ther.* **2007**, *115*, 1–12.
(17) Ham, S. W.; Carr, B. I. Cell division cycle 25 (Cdc25) phosphatase inhibitors as antitumor agents. *Drug Des. Rev.* **2004**, *1*, 123–132.
(18) Prevost, G. P.; Brezak, M.-C.; Goubin, F.; Mondesert, O.; Galcera, M.-O.; Quaranta, M.; Alby, F.; Lavergne, O.; Ducommun, B. *Prog. Cell Cycle Res.* **2003**, *5*, 225–234.
(19) Lazo, J. S.; Aslan, D. C.; Southwick, E. C.; Cooley, K. A.; Ducruet, A. P.; Joo, B.; Vogt, A.; Wipf, P. Discovery and biological evaluation of a new family of potent inhibitors of the dual specificity protein phosphatase Cdc25. *J. Med. Chem.* **2001**, *44*, 4042–4049.
(20) Sohn, J.; Kiburz, B.; Li, Z.; Deng, L.; Safi, A.; Pirrung, M. C.; Rudolph, J. Inhibition of Cdc25 phosphatases by indolyldihydroxyquinones. *J. Med. Chem.* **2003**, *46*, 2580–2588.
(21) Brault, L.; Denancé, M.; Banaszak, E.; Maadidi, S. E.; Battaglia, E.; Bagrel, D.; Samadi, M. Synthesis and biological evaluation of dialkylsubstituted maleic anhydrides as novel inhibitors of Cdc25 dual specificity phosphatases. *Eur. J. Med. Chem.* **2007**, *42*, 243–247.
(22) Huang, W.; Li, J.; Zhang, W.; Zhou, Y.; Xie, C.; Luo, Y.; Li, Y.; Wang, J.; Li, J.; Lu, W. Synthesis of miltirone analogues as inhibitors of Cdc25 phosphatases. *Bioorg. Med. Chem. Lett.* **2006**, *16*, 1905–1908.
(23) Brun, M.-P.; Braud, E.; Angotti, D.; Mondésert, O.; Quaranta, M.; Montes, M.; Miteva, M.; Gresh, N.; Ducommun, B.; Garbay, C. Design, synthesis, and biological evaluation of novel naphthoquinone derivatives with Cdc25 phosphatase inhibitory activity. *Bioorg. Med. Chem.* **2005**, *13*, 4871–4879.
(24) Contour-Galcéra, M.-O.; Lavergne, O.; Brezak, M.-C.; Ducommun, B.; Prévost, G. Synthesis of small molecule CDC25 phosphatases inhibitors. *Bioorg. Med. Chem. Lett.* **2004**, *14*, 5809–5812.
(25) Lazo, J. S.; Nemoto, K.; Pestell, K. E.; Cooley, K.; Southwick, E. C.; Mitchell, D. A.; Furey, W.; Gussio, R.; Zaharevitz, D. W.; Joo, B.; Wipf, P. Identification of a potent and selective pharmacophores for Cdc25 dual specificity phosphatase inhibitors. *Mol. Pharmacol.* **2002**, *61*, 720–728.
(26) Lavecchia, A.; Cosconati, S.; Limongelli, V.; Novellino, E. Modeling of Cdc25B dual specificity protein phosphatase inhibitors: docking of ligands and enzymatic inhibition mechanism. *ChemMedChem* **2006**, *1*, 540–550.
(27) Park, H.; Carr, B. I.; Li, M.; Ham, S. W. Fluorinated NSC as a Cdc25 inhibitor. *Bioorg. Med. Chem. Lett.* **2007**, *17*, 2351–2354.
(28) Warren, G. L.; Andrews, C. W.; Capelli, A.-M.; Clarke, B.; LaLonde, J.; Lambert, M. H.; Lindvall, M.; Nevins, N.; Semus, S. F.; Senger, S.; Tedesco, G.; Wall, I. D.; Woolven, J. M.; Peishoff, C. E.; Head, M. S. *J. Med. Chem.* **2006**, *49*, 5912–5931.
(29) Zou, X.; Sun, Y.; Kuntz, I. D. Inclusion of solvation in ligand binding free energy calculations using generalized-Born model. *J. Am. Chem. Soc.* **1999**, *121*, 8033–8043.
(30) Shoichet, B. K.; Leach, A. R.; Kuntz, I. D. Ligand solvation in molecular docking. *Proteins* **1999**, *34*, 4–16.
(31) With respect to the numbering scheme for the amino acids, we followed those used in the X-ray crystallographic studies of Cdc25A (ref 14) and Cdc25B (ref 15).
(32) Baker, D.; Sali, A. Protein structure prediction and structural genomics. *Science* **2001**, *294*, 93–96.
(33) Bairoch, A.; Apweiler, R. The SWISS-PROT protein sequence data bank and its supplement TrEMBL in 1999. *Nucleic Acids Res.* **1999**, *27*, 49–54.

(34) Thompson, J. D.; Higgins, D. G.; Gibson, T. J. CLUSTAL W: improving the sensitivity of progressive multiple sequence alignment through sequence weighting, position-specific gap penalties and weight matrix choice. *Nucleic Acids Res.* **1994**, *22*, 4673–4680.

(35) Sali, A.; Blundell, T. L. Comparative protein modelling by satisfaction of spatial restraints. *J. Mol. Biol.* **1993**, *234*, 779–815.

(36) Fiser, A.; Do, R. K. G.; Sali, A. Modeling of loops in protein structures. *Protein Sci.* **2000**, *9*, 1753–1773.

(37) Sippl, M. J. Recognition of errors in three-dimensional structures of proteins. *Proteins* **1993**, *17*, 355–362.

(38) Morris, G. M.; Goodsell, D. S.; Halliday, R. S.; Huey, R.; Hart, W. E.; Belew, R. K.; Olson, A. J. Automated docking using a Lamarckian genetic algorithm and an empirical binding free energy function. *J. Comput. Chem.* **1998**, *19*, 1639–1662.

(39) Park, H.; Lee, J.; Lee, S. Critical assessment of the automated AutoDock as a new docking tool for virtual screening. *Proteins* **2006**, *65*, 549–554.

(40) Jeffrey, G. A. *An Introduction to Hydrogen Bonding*; Oxford University Press: Oxford, U.K., 1997.

(41) Lipinski, C. A.; Lombardo, F.; Dominy, B. W.; Feeney, P. J. Experimental and computational approaches to estimate solubility and permeability in drug discovery and development settings. *Adv. Drug Delivery Rev.* **1997**, *23*, 3–25.

(42) Gasteiger, J.; Marsili, M. Iterative partial equalization of orbital electronegativity—a rapid access to atomic charges. *Tetrahedron* **1980**, *36*, 3219–3228.

(43) Mehler, E. L.; Solmajer, T. Electrostatic effects in proteins: comparison of dielectric and charge models. *Protein Eng.* **1991**, *4*, 903–910.

(44) Stouten, P. F. W.; Frömmel, C.; Nakamura, H.; Sander, C. An effective solvation term based on atomic occupancies for use in protein simulations. *Mol. Simul.* **1993**, *10*, 97–120.

(45) Kang, H.; Choi, H.; Park, H. Prediction of molecular solvation free energy based on the optimization of atomic solvation parameters with genetic algorithm. *J. Chem. Inf. Model.* **2007**, *47*, 509–514.

(46) Tamura, K.; Southwick, E. C.; Kerns, J.; Rosi, K.; Carr, B. I.; Wilcox, C.; Lazo, J. S. Cdc25 inhibition and cell cycle arrest by a synthetic thioalkyl vitamin K analogue. *Cancer Res.* **2000**, *60*, 1317–1325.

(47) Osada, S.; Osada, K.; Carr, B. I. Tumor cell growth inhibition and extracellular signal-regulated kinase (ERK) phosphorylation by novel K vitamins. *J. Mol. Biol.* **2001**, *314*, 765–772.

(48) Rice, R. L.; Rusnak, J. M.; Yokokawa, F.; Yokokawa, S.; Messner, D. J.; Boynton, A. L.; Wipf, P.; Lazo, J. S. A targeted library of small-molecule, tyrosine, and dual-specificity phosphatase inhibitors derived from a rational core design and random side chain variation. *Biochemistry* **1997**, *36*, 15965–15974.

JM701157G